

P. R. PASLAY

Professor,
Division of Engineering,
Brown University,
Providence, R. I.

C. H. WELLS

G. R. LEVERANT

L. H. BURCK

Advanced Materials Research
and Development Laboratory,
Pratt & Whitney Aircraft,
Middletown, Conn.

Creep of Single Crystal Nickel-Base Superalloy Tubes Under Biaxial Tension

An analysis of the statically indeterminate problem of the creep of a biaxially loaded, anisotropic hollow cylinder is presented. The anisotropy of the material leads to a nonuniform axial stress distribution which is evaluated by numerical techniques. Single crystal, tubular specimens of a nickel-base alloy were creep-tested at 1400 deg F with an <001> crystallographic axis nearly coincident with the tube axis in order to evaluate the theoretical analysis. Comparison of predicted and measured creep rates shows fair agreement.

Introduction

THE incorporation of nickel-base superalloy single crystals into design requires consideration of their anisotropy. Earlier work [1]¹ has shown that the planar slip associated with creep under certain combinations of stress and temperature occurs on {111} planes in the <112> directions. An analysis of the variation of the primary creep rate with orientation of the crystallographic axes relative to a uniaxial tensile stress was in reasonably good agreement with experimental measurements.

¹ Numbers in brackets designate References at end of paper.

Contributed by the Applied Mechanics Division and presented at the Applied Mechanics Conference, The University of Pennsylvania, Philadelphia, Pa., June 23-25, 1971, of THE AMERICAN SOCIETY OF MECHANICAL ENGINEERS.

Discussion on this paper should be addressed to the Editorial Department, ASME, United Engineering Center, 345 East 47th Street, New York, N. Y. 10017, and will be accepted until October 20, 1971. Discussion received after the closing date will be returned. Manuscript received by ASME Applied Mechanics Division, May 25, 1970. Paper No. 71-APM-1.

Testing was conducted under conditions resulting in planar slip (1400 deg F, stress in the vicinity of 100,000 psi).

The application of such materials frequently involves biaxial loading, and in this case the creep rate is governed both by the orientation of the crystallographic axes and the ratio of the applied stresses. In general such loading would not result in axisymmetric deformation. However, since the application of this material is frequently to a hollow airfoil grown with its span along the [001] axis of symmetry, and in order to simplify the analysis, only the axisymmetric case is treated here. The theoretical formulation presented in [1] is applied to the case of a thin-walled tube subjected to combined internal pressure and axial loading. Because the longitudinal stress distribution in a biaxially loaded single crystal tube is not statically determinate, this case serves to illustrate the design problem and allows a relatively simple experimental evaluation of the analysis.

Theoretical Considerations

The theory presented in [1] superposes deformation rates associated with each of the <112> directions on the {111} planes. As a result 12 deformation rates are summed. The deformation

Nomenclature

C = constant in creep law, see (2)
 d_{zz} = axial deformation rate
 F = axial load on thin-walled tube, see Fig. 2
 p = internal pressure on thin-walled tube, see Fig. 2
 r, θ, z = cylindrical coordinate system, see Fig. 2
 R = radius of thin-walled tube, see Fig. 2
 t = wall thickness of thin-walled tube, see Fig. 2

x = Cartesian coordinates parallel to crystallographic directions
 $1, 2, 3, 4$ = vectors defining {111} planes, see Fig. 1
 $1, 2, 3, 4$ = indexes referring to <112> slip directions on the {111} planes, see Fig. 1
 β = constant in creep law, see (2)
 $\dot{\gamma}_{ij}$ = engineering shear strain rate on i th {111} plane in the j th <112> direction, see Fig. 1

σ_A = average axial stress on thin-walled tube, see (7)
 σ_θ = constant hoop stress, equal to pR/t , see Fig. 2
 $\sigma_z, \sigma_z(\theta)$ = axial stress in thin-walled tube which depends on angular position θ , see Fig. 2
 τ_{ij} = shear stress component acting on the i th {111} plane parallel to the j th <112> direction

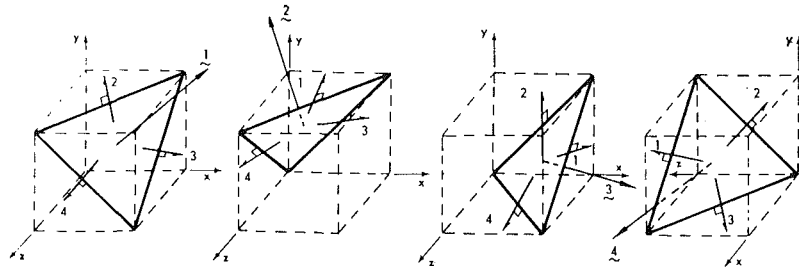


Fig. 1 Unit cubes showing four $\{111\}$ planes and corresponding $\langle 112 \rangle$ directions with respect to crystallographic axes x, y, z

rate on each system is found by determining the component of shearing stress on the plane in the direction of the system. This shear stress is denoted as follows:

$$\tau_{ij} = \text{component of shear stress on the } i\text{th plane in } j\text{th direction} \quad (1)$$

The numbering system used here for the various planes and directions is indicated in Fig. 1. The corresponding deformation rates associated with the slip systems are then, in terms of the material parameters C and β , given by,

$$\dot{\gamma}_{ij} = C \frac{\tau_{ij}}{|\tau_{ij}|} (e^{\beta|\tau_{ij}|} - 1) \quad (2)$$

The only stresses which are taken into account in this analysis are the hoop tension σ_θ and the axial stress σ_z ; see Fig. 2. Although one $\langle 100 \rangle$ crystallographic axis is parallel to the cylinder axis, the other $\langle 100 \rangle$ axes form various angles with the local radial direction. As a result, the anisotropic behavior of the crystal causes σ_z to vary with θ while σ_θ is approximated to be simply pR/t everywhere. Let the radial line θ equal zero be a $\langle 100 \rangle$ axis. Under these circumstances denote σ_z as $\sigma_z(\theta)$ and the τ_{ij} stresses become,

$$\begin{aligned} 3\sqrt{2}\tau_{12} &= 3\sqrt{2}\tau_{43} = (pR/t)(-\cos^2\theta + 2\sin^2\theta - \cos\theta\sin\theta) - \sigma_z(\theta) \\ 3\sqrt{2}\tau_{13} &= 3\sqrt{2}\tau_{42} = (pR/t)(+2\cos^2\theta - \sin^2\theta - \cos\theta\sin\theta) - \sigma_z(\theta) \\ 3\sqrt{2}\tau_{14} &= 3\sqrt{2}\tau_{41} = (pR/t)(-\cos^2\theta - \sin^2\theta + 2\cos\theta\sin\theta) + 2\sigma_z(\theta) \\ 3\sqrt{2}\tau_{21} &= 3\sqrt{2}\tau_{34} = (pR/t)(-\cos^2\theta + 2\sin^2\theta + \cos\theta\sin\theta) - \sigma_z(\theta) \\ 3\sqrt{2}\tau_{23} &= 3\sqrt{2}\tau_{32} = (pR/t)(-\cos^2\theta - \sin^2\theta - 2\cos\theta\sin\theta) + 2\sigma_z(\theta) \\ 3\sqrt{2}\tau_{24} &= 3\sqrt{2}\tau_{31} = (pR/t)(+2\cos^2\theta - \sin^2\theta + \cos\theta\sin\theta) - \sigma_z(\theta) \end{aligned} \quad (3)$$

In this case, at any value of θ , the total axial deformation rate d_{zz} may be expressed from (3) using (2) and the results given in [1] as

$$3d_{zz} = \sqrt{2}(-\dot{\gamma}_{12} - \dot{\gamma}_{13} + 2\dot{\gamma}_{14} - \dot{\gamma}_{21} + 2\dot{\gamma}_{23} - \dot{\gamma}_{24}) \quad (4)$$

Now, for every value of θ , the value of d_{zz} must be the same at any time since the ends of the cylinder are constrained from distortion. A computer program was developed which for a specified pR/t finds the distribution $\sigma_z(\theta)$ which yields a uniform d_{zz} for $0 < \theta < 45$ deg. This completely describes the $\sigma_z(\theta)$ distribution as

$$\sigma_z(\theta) = \sigma_z(-\theta) \text{ and } \sigma_z(\theta) = \sigma_z(\theta + \pi/2) \quad (5)$$

The predicted axial primary creep rate is then d_{zz} for the pressure p and axial load F given by

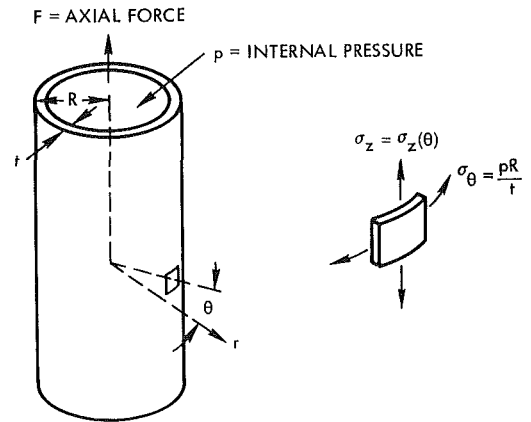


Fig. 2 Hollow cylinder: configuration, loading, and stresses

$$F = 8Rt \int_0^{\pi/4} \sigma_z(\theta) d\theta \quad (6)$$

The nominal axial stress σ_A which is

$$\sigma_A = F/2\pi Rt = 4/\pi \int_0^{\pi/4} \sigma_z(\theta) d\theta \quad (7)$$

is also of interest.

To demonstrate some typical results the constants in (2) are taken from the experiments in [1] for 1400 deg F as

$$\begin{aligned} C &= 2.86 \times 10^{-12} (\text{hr})^{-1} \\ \beta &= 0.00045 \quad (\text{psi})^{-1} \end{aligned} \quad (8)$$

and $\sigma_z(\theta)$ curves are given for σ_θ equal to 0, 50, and 100 ksi and three different axial initial creep rates in Fig. 3. These results are summarized in Fig. 4, where the nominal axial stress σ_A is plotted as a function of d_{zz} for various values of σ_θ . The parameters appearing in Fig. 4 are easily measured, so that this result is suitable for evaluation of the creep theory by comparison with experimental results.

Experimental Program

In order to evaluate the theoretical predictions, a series of five single crystal specimens of the carbide-free nickel-base superalloy Mar-M200 [2] was tested in creep at 1400 deg F under several combinations of internal pressure and axial load. Test specimens were 1/2-in. ID, 0.015-in. wall, 1.8-in. gage length tubes oriented with the longitudinal specimen axis within $7\frac{1}{2}$ deg of the $[001]$ crystallographic axis. Axial load was applied in a deadweight creep machine, and internal pressurization by argon gas regulated within ± 100 psi. The specimen and grips were heated in a resistance furnace, and the wall temperature maintained within ± 2 deg of 1400 deg F.

The test assembly is shown in Fig. 5. The left and right-

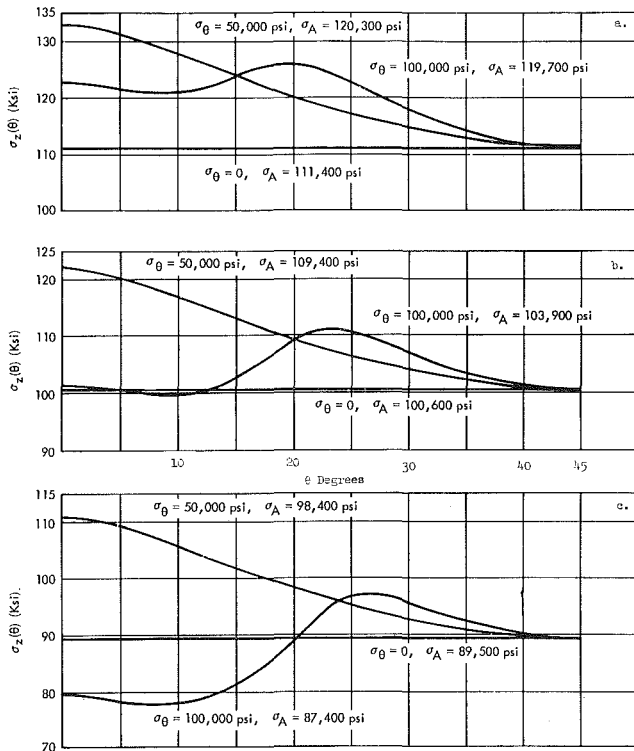


Fig. 3 $\sigma_z(\theta)$ for hoop stresses of 0, 50, and 100 ksi for axial primary creep rates of (a) 0.05 (hr)^{-1} ; (b) 0.005 (hr)^{-1} ; (c) 0.0005 (hr)^{-1}

hand threads on each collar compress the hollow O-rings, thus effecting a pressure seal when the collar is tightened against the pull rod. This arrangement avoids the application of torque to the specimen gage length. Axial alignment is obtained through ground surfaces on the pull rods which fit snugly into the bore of the test specimen. Axial strains were measured with a linear variable differential transformer suspended outside the furnace by alumina extension rods connected to each collar. No attempt was made to measure circumferential strains during the test.

The primary creep rate of the biaxially stressed hollow cylinders decreased continuously with time. For this reason, the creep rate at zero time (initial creep rate) was chosen to compare with the predicted axial creep rate. In addition, the initial creep rate is most representative of creep under conditions of minimal interaction of dislocations on intersecting glide systems, a condition which is assumed in the analytical representation.

The measured and predicted axial creep rates are given in Table 1 for each specimen along with the applied stresses and misorientation of the cylinder and crystallographic axes.

Discussion

Reasonable agreement is obtained between the predicted and measured axial creep rates, Table 1. It has been demonstrated in previous papers [1,2] that the primary creep rate of this material at the same temperature and under uniaxial loading is a function of the angle between the $\langle 001 \rangle$ axis and the loading axis. The analytical treatment for the biaxial case assumes the $\langle 001 \rangle$ axis is coincident with the cylinder axis; however, this was not true for the specimens tested. This factor may be partially responsible for the discrepancies between the predicted and measured creep rates.

In applying the analytical procedures developed in this paper, as well as in reference [1], one must determine the nature of the

Table 1 Comparison of the measured and predicted initial axial creep rates

Specimen Number	σ_θ , hoop stress (ksi)	σ_A , axial stress (ksi)	Measured axial creep rate $(\text{hr})^{-1}$	Predicted axial creep rate ^a $(\text{hr})^{-1}$	Angle between $\langle 001 \rangle$ axis and the cylinder axis (deg)
1	50	100	0.0009	0.0007	4.5
2	100	100	0.0050	0.0030	7.5
3	0	100	0.0055	0.0080	6
4	100	50	0	0	2.5
5	84.5	84.5	0.0005	0.00012	5

^aBased on material parameters given in equation (8).

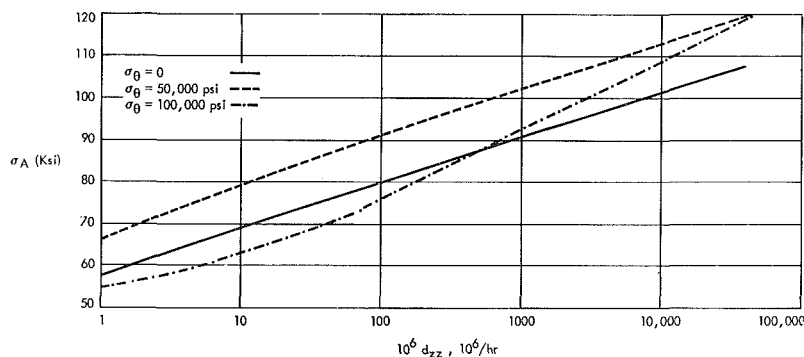


Fig. 4 Nominal axial stress σ_A versus the axial primary creep rate \dot{d}_{zz} for indicated values of hoop stress σ_θ

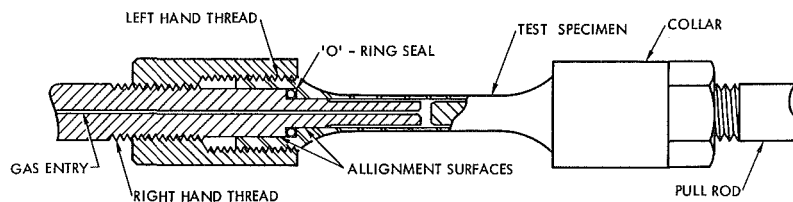


Fig. 5 Experimental arrangement of specimen and adapters

anisotropic behavior of the material at the particular temperature of interest. For example, whereas these analyses are valid for creep at temperatures around 1400 deg F, at which shear occurs almost exclusively in $\langle 112 \rangle$ directions, recent work [3] has shown that both $\langle 110 \rangle$ and $\langle 112 \rangle$ shear directions are operative around 1600 deg F. In the latter case, the analyses should be modified to account for the simultaneous operation of two shear directions.

Conclusions

A theoretical treatment has been developed to analyze the statically indeterminate problem of the creep of an anisotropic hollow cylinder under biaxial loading. Reasonable agreement between theory and experiment was obtained for the creep of nickel-base alloy single crystals at 1400 deg F.

Acknowledgment

The authors wish to thank R. K. Smith for his valuable assistance in conducting the testing.

References

- 1 Paslay, P. R., Wells, C. H., and Leverant, G. R., "An Analysis of Primary Creep of Face-Centered Cubic Crystals," to be published in the *JOURNAL OF APPLIED MECHANICS*.
- 2 Leverant, G. R., and Kear, B. H., "The Mechanism of Creep in Gamma Prime Precipitation-Hardened Nickel-Base Alloys at Intermediate Temperatures," *Metallurgical Transactions*, Vol. 1, 1970, p. 491.
- 3 Leverant, G. R., Oblak, J. M., and Kear, B. H., unpublished research, Pratt & Whitney Aircraft, Middletown, Conn.